



# Journal of Applied Sciences

ISSN 1812-5654

**science**  
alert

**ANSI***net*  
an open access publisher  
<http://ansinet.com>

## Effect of Curvature Ratio on Cooperating Double-Diffusive Convection in Vertical Annular Cavities

<sup>1</sup>Noureddine Retiel, <sup>2</sup>El-Hadi Bouguerra and <sup>3</sup>Mohamed Aïchouni

<sup>1</sup>Department of Mechanical Engineering, University of Mostaganem, B.P. 188, Mostaganem Algeria

<sup>2</sup>Department of Mechanical Engineering, University of Blida, Soumâa, B.P. 270, Blida Algeria

<sup>3</sup>Department of Mechanical Engineering, Hail College of Technology, P.O. Box 7469, Hail, KSA

---

**Abstract:** A numerical study is performed on double diffusive natural convection fluid flow in a vertical closed annulus. Uniform temperature and concentration are imposed across the vertical walls. The aim of this study is to present numerical results on the cooperating double diffusive convection phenomena in a vertical annular cavity under different curvature ratio ( $K = 1-20$ ). The numerical procedure used is based on the solution of the momentum equations coupled with the energy and concentration equations. A finite-volume method is adopted to solve the governing equations. The analysis of the numerical results obtained concerns the study of the effects of the buoyancy ratio governing the physical problem on the heat and mass transfer characteristics and on the flow structure. Double diffusive flow structures have been successfully simulated under certain conditions.

**Key words:** Natural convection, thermosolutal, annular cavity, concentration, temperature, mass transfer

---

### INTRODUCTION

Fluid flow phenomena under the simultaneous influence of temperature and concentration gradients occur very frequently in nature and in technological systems. In nature, water flows in human bodies are mainly driven by the effects of temperature and concentration of dissolved materials. Atmospheric flows occurring in air and oceans can be initiated by temperature and concentration differences. Evaporative cooling of high temperature energetic systems, solidification and crystal growth from flow phases, drying processes and liquid gas storage are just few examples in the technological world.

Natural convection resulting from thermal and solutal buoyancy force in rectangular cavities has been extensively investigated in the open literature (Gebhart and Pera, 1971; Bejan, 1985; Lin *et al.*, 1990). The experimental studies presented by Kamotani *et al.* (1985), show that when a stable stratified solution is heated from one side, multicellular flow structures are observed. This has been confirmed by the numerical simulations presented by Bennacer and Gobin (1996) and Gobin and Bennacer (1996). However, the double diffusive convection in cylindrical cavities and particularly in vertical annular cavities has not received enough attention. Most of studies presented in the open literature

concern thermosolutal natural convection in concentric annular cavities at low and moderate Lewis number ( $Le$  is defined as the ratio of the thermal diffusivity to the molecular diffusivity)  $Le = 1-10$  presented by Shipp *et al.* (1993a). These conditions refer to binary gases. The high Lewis number (of the order of 100) which refers to thermosolutal convection in liquids leads to more complex flow situations. This has been considered as an interesting challenge from an experimental and numerical stand points. Numerical predictions of the thermosolutal convection at high Lewis numbers obtained by Han and Kuehn (1991) in vertical rectangular enclosure or by Bennacer *et al.* (2000), in vertical annular cavities in porous medium where indicated that under certain conditions a multicellular flow regime occurs. The transition from a monocellular to a multicellular flow regime is still subject to a scientific debate. Among the most recent studies are those of Bahloul *et al.* (2006) and concerns an analytical and numerical study of the natural convection of a two-component fluid in porous media bounded by tall concentric vertical cylinders.

The objective of the present study is to determine the influence of the induced solutal buoyancy forces (cooperating forces) on the flow structures and heat transfer rates associated to the natural convection of an initially uniform concentration fluid contained in an enclosure with heated and cooled walls. The double

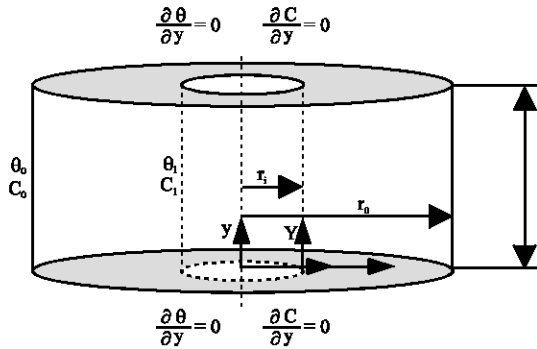


Fig. 1: Shallow annulus physical domain

diffusive convection phenomena in an annular cavities under different geometrical conditions (radii ratio  $K = 1$  to  $20$ ) has been considered numerically. The numerical predictions presented here concern a large number of parameters and allow the study of the flow structure in order to give more insight into the formation of multicellular flow regime and its impact on heat and mass transfer rates.

**Physical problem and numerical model:** The physical problem under consideration is presented in Fig. 1. It consists of an annular cavity, set vertically, where both cylindrical walls are isothermal and at a uniform concentration. The inner wall temperature is higher than the outer one ( $T_i > T_o$ ). The configurations considered in the present study with cooperating horizontal gradients (the thermal and solutal convection cooperate) are generated by prescribing a lower concentration at the hot (inner) wall than at the cold (outer) one ( $C_i < C_o$ ). The upper and lower ending walls are assumed to be both insulated and adiabatic and no-slip dynamic boundary conditions are imposed at the walls.

The main usual hypotheses of incompressible and laminar flow are considered. The binary fluid is assumed to be Newtonian and its density is supposed to be constant, except in the driving term of the Navier-Stokes equation, where it varies linearly with the local temperature and solute mass fraction (Boussinesq approximation).

$$\rho(T, C) = \rho_0 [1 - \beta_T (T - T_0) - \beta_C (C - C_0)]$$

With  $\beta_T > 0$  and  $\beta_C < 0$  are the thermal and concentration expansion coefficients:

$$\beta_T = -\frac{1}{\rho} \left( \frac{\partial \rho}{\partial \theta} \right)_p \quad \beta_C = -\frac{1}{\rho} \left( \frac{\partial \rho}{\partial C} \right)_p$$

According to Le Quéré (1987), the use of the thermal diffusive velocity as a reference reported to the width of the cavity ( $\alpha/\Delta r$ ) has been found to be a source of numerical difficulties at high Rayleigh numbers. Instead the use of the convective velocity ( $\alpha\sqrt{Ra_t}/\Delta r$ ) as a reference was shown to be suitable for natural convection in cavities.

In the present study the governing equations were made dimensionless by using the radii difference as the reference length,  $\Delta r = r_o - r_i$ .

where:

$$R = \frac{r - r_i}{\Delta r} = \frac{r}{\Delta r} - e \quad Y = \frac{y}{\Delta r}$$

$$U = \frac{\Delta r}{\alpha\sqrt{Ra_t}} u \quad V = \frac{\Delta r}{\alpha\sqrt{Ra_t}} v$$

$$P = \frac{\Delta r^2}{\rho\alpha^2 Ra_t} p$$

All reference conditions are taken at the mean value. Thus the dimensionless temperature and concentration become normalized :

$$T = \frac{\theta - \theta_r}{\theta_i - \theta_o} \quad S = \frac{C - C_r}{C_i - C_o}$$

where:  $\theta_r = \frac{\theta_i + \theta_o}{2}$  and  $C_r = \frac{C_i + C_o}{2}$

The dimensionless governing parameters present in equations are defined as:

The Prandtl number:  $Pr = \nu/\alpha$   
 The Lewis number:  $Le = \alpha/D$   
 The thermal Rayleigh number:  $Ra_t = \frac{g\beta_T \Delta \theta \Delta r^3}{\nu\alpha}$

The solutal Rayleigh number:  $Ra_c = \frac{g\beta_C \Delta C \Delta r^3}{\nu\alpha}$

The buoyancy ratio:  $N = Ra_c / Ra_t$

The geometric system parameters are defined as:

$$A_r = H/\Delta r \quad K = r_o/r_i$$

With the above mentioned dimensionless variables and for axisymmetric unsteady natural convection, the governing partial differential equations for continuity, momentum, energy and species can be written as:

Continuity equation for mass conservation:

$$\frac{\partial[(R+e)U]}{(R+e)\partial R} + \frac{\partial V}{\partial Y} = 0$$

Radial momentum equation:

$$U \frac{\partial U}{\partial R} + V \frac{\partial U}{\partial Y} = -\frac{\partial P}{\partial R} + \frac{Pr}{\sqrt{Ra_t}} \left[ \nabla^2 U - \frac{U}{(R+e)^2} \right]$$

Axial momentum equation:

$$U \frac{\partial V}{\partial R} + V \frac{\partial V}{\partial Y} = -\frac{\partial P}{\partial Y} + \frac{Pr}{\sqrt{Ra_t}} \nabla^2 V + Pr(T + NS)$$

Thermal energy equation:

$$U \frac{\partial T}{\partial R} + V \frac{\partial T}{\partial Y} = \frac{1}{\sqrt{Ra_t}} \nabla^2 T$$

Mass species

$$U \frac{\partial S}{\partial R} + V \frac{\partial S}{\partial Y} = \frac{1}{Le\sqrt{Ra_t}} \nabla^2 S$$

where  $\nabla^2 = \frac{\partial}{\partial R} \left( R \frac{\partial}{\partial R} \right) + \frac{\partial}{\partial Y^2}$

The dimensionless boundary conditions for the physical system considered are:

$$\begin{aligned} \text{At } R = 0; & \quad T_i = 0.5 \text{ and } S_i = -0.5 \\ \text{At } R = 1; & \quad T_o = -0.5 \text{ and } S_o = 0.5 \end{aligned}$$

The top and bottom walls are adiabatic and impermeable: at  $Y = 0, Ar \quad \frac{\partial T}{\partial Y} = \frac{\partial S}{\partial Y} = 0$

The velocity boundary conditions are non-slip and no fluid enters or exists the annulus:

$$\text{At } R = 0,1 \quad Y = 0,1 \quad \text{and} \quad U = V = 0$$

**Numerical procedure:** The numerical method is based on the SIMPLER (Semi Implicit Method for Pressure Equation Revised) ; developed by Patankar (1980). The governing equations are spatially discretized over a staggered grid using the finite difference method and then integrated over control volumes. The SIMPLER algorithm is an iterative scheme, which consists of correcting velocities a priori estimated with the momentum equations. As the iterative process converges, the velocities will fit the

pressure correction equations derived from the continuity equation are solved with a direct method, while for the other equations (momentum, energy and concentration), a Tri-Diagonal Matrix Algorithm is used. In order to improve the convergence of the iterative procedure, an under-relaxation of the equations is necessary. The convergence of the algorithm is reached when the residual of the momentum equations is less than  $10^{-5}$ .

The physical domain is discretized into a non-uniform grid, which ensures grid spacing close to the walls and a coarser mesh system in the core region.

## RESULTS

The study describes the numerical results of the steady state double diffusion in annular cavities with different aspect ratios. The cavity filled with water ( $Pr = 7$ ) is subject to aiding thermal and solutal buoyancy forces. The Lewis number is set to  $Le = 100$  representing the case where thermal diffusivity is much greater than the solutal diffusivity. These conditions have been considered in most experimental and numerical studies published in the open literature (Bennacer and Gobin, 1996, 2000; Gobin and Bennacer, 1996; Han and Kuhen, 1991; Retiel, 1995). The solutal Rayleigh number vary from  $2 \times 10^5$  to  $50 \times 10^5$  for a thermal Rayleigh number set at a fixed value of  $10^5$ . Comprehensive information on velocity, temperature and concentration are obtained and discussed. Particular interest has been focused on the effects of the buoyancy ratio and the curvature ratio on the heat and mass transfer rates and on subsequent the flow structure regimes.

In order to obtain accurate solutions for wall heat and mass transfer and to optimize the numbers of control volumes, non-uniform grid spacing were used. The numerical grid  $51 \times 51$  used to carry the present numerical study.

**Effect of the buoyancy ratio:** This section describes the numerical results of the steady state double diffusion in annular cavities with different aspect ratios. The cavity filled with water ( $Pr = 7$ ) is subject to aiding thermal and solutal buoyancy forces. The Lewis number is set to  $Le = 100$  representing the case where thermal diffusivity is much greater than the solutal diffusivity. These conditions have been considered in most experimental and numerical studies published in the open literature. The thermal Rayleigh number set at a fixed value of  $10^5$  for a solutal Rayleigh number vary from  $2.0 \times 10^5$  to  $50 \times 10^5$ . Comprehensive information on velocity, temperature and concentration are obtained and discussed. Particular interest has been focused on the effects of the buoyancy ratio on the heat and mass transfer rates and on subsequent the flow structure regimes.

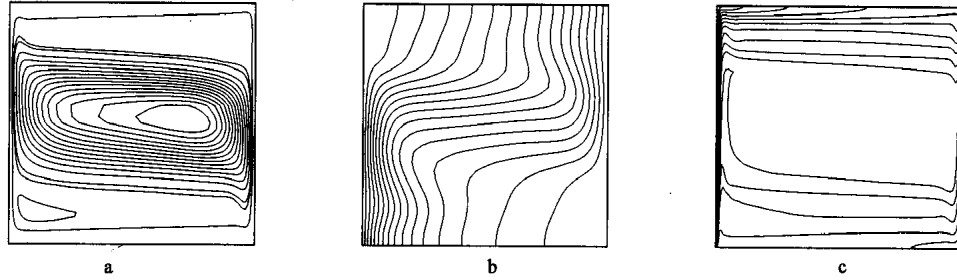


Fig. 2: Flow structure and temperature and concentration distribution, for equivalent buoyancy forces ( $N = 20$ ,  $Ra_t = 10^5$ ,  $Pr = 7$ ,  $Le = 100$ ,  $K = 2$ )

In order to study the effect of the buoyancy ratio we consider a square cavity ( $Ar = 1$ ) with a curvature ratio  $K = 2$ . The buoyancy ratio varied from the value of 2 to 50 corresponding to the most extreme cases of aiding buoyancy driven phenomena. The detailed numerical predictions presented by Retiel (1995), show that for low buoyancy ratio ( $N < 10$ ), thermal buoyancy is dominant and the flow structure of is unicellular and similar to pure thermal convection. The solutal driven flow is mainly localized in the vicinity of the acting walls. The core of the cavity is occupied by a stratified thermal flow a constant concentration.

For similar thermal and solutal buoyancy forces ( $N = 20$ ), the stagnant core flow structure start moving leading to an increase of the temperature gradients in the core region and horizontal isotherms near the active walls (Fig. 2b). This characterizes flow regions with low velocities where heat and mass transfers are mainly conductive in the horizontal sense. The streamlines presented in Fig. 2a, show clearly these stagnant flow regions. This can be explained by the fact that the central thermal cell opposes to the mass diffusion towards the central region.

A stratified region of concentration develops in the wall vicinity. This flow zone occupies wider region as the buoyancy ratio,  $N$  increases. The width of this region is about 20% of  $H$  for  $N = 10$  and 60% for  $N = 20$ . Figure 3 presents the axial velocity profiles at  $R = 0.5$  for buoyancy ratio  $N = 5, 10, 20$  and  $50$ .

When the thermal convection is dominant ( $N = 5$ ), the solutal buoyancy force is negligible because of the Lewis number is set to  $Le = 100$  representing the case where thermal diffusivity is much greater than the solutal diffusivity. For comparable buoyancy forces ( $N = 20$ ), the solutal boundary layer superimposes between the convective thermal flow at the core region and the heated walls. For dominant solutal buoyancy ( $N = 50$ ), the flow is suppressed by the stable stratification of concentration which develops in the cavity. The flow is mainly a boundary layer type in the vicinity of the vertical walls.

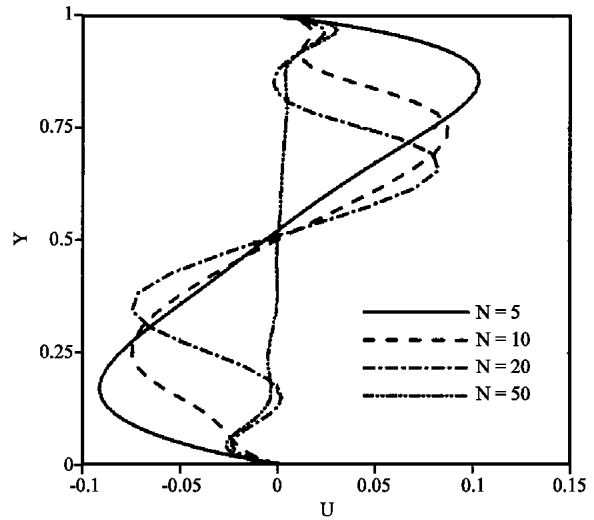


Fig. 3: Axial velocity profile at  $R = 0.5$  (for  $Ra_t = 105$ ,  $Le = 100$ ,  $Pr = 7.0$ ,  $K = 2$ ,  $Ar = 1$ )

This can be clearly seen from the velocity profiles at  $R = 0.5$  in Fig. 3 and the streamlines presented in Fig. 4a. The heat transfer is mainly convective which is presented by horizontal isotherms (Fig. 4b).

A brief analysis of the flow structure for moderate and high buoyancy ratios ( $N = 20$  and  $50$ ) respectively at a fixed Lewis number  $Le = 100$  (Fig. 2 and 3) may contribute to the understanding of the decrease of the heat transfer along the heated wall. From these figures, the following observations can be made:

For moderate buoyancy ratio ( $N = 20$ ), the flow is limited to the central part of the cavity (Fig. 2a) and the top and bottom regions are almost stagnant zones characterized by low flow velocities. This will be explained later and shown to be due to the relative importance of the thermal and solutal effects. For high buoyancy ratios, the flow concerns mainly a very thin boundary layers along the active walls (Fig. 3).

The temperature field is consistent with the flow structure. For  $N = 20$ , the stratification of the motionless

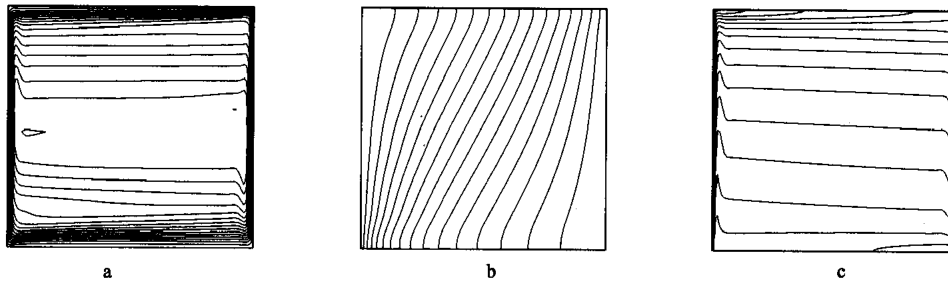


Fig. 4: Flow structure and temperature and concentration distribution, for dominant solutal buoyancy forces ( $N = 50$ ,  $Ra_t = 10^5$ ,  $Pr = 7$ ,  $Le = 100$ ,  $K = 2$ )

central cell leads to a conduction like flow behavior. This can be seen from the parallel isotherms to the vertical walls (Fig. 2b). For  $N = 50$ , the temperature field seems not to be affected by the fluid flow (illustrated by practically parallel isotherms (Fig. 6b). The heat transfer can be considered as purely conductive.

The concentration field is characterized by thin boundary layers with two stratified zones at the top and bottom and an homogeneous cell at the center (Fig. 2c). As the buoyancy ratio  $N$  increases, the concentration is stratified over the whole of the height of the cavity (Fig. 3c).

**Curvature ratio effect:** We consider different cavities where radii ratio vary from  $K = 1$  to  $K = 20$ . More, to compare the flow in annular ( $K > 1$ ) and rectangular ( $K \approx 1$ ) cavities, we consider a case where the radii ratio nearly equal to unity. Numerical results present with  $Ra_t = 10^5$ ,  $Pr = 7$ ,  $Le = 100$  and  $Ar = 1$ .

Flow structure with different radii ratio, display than unlike to rectangular cavity who present a symmetric aspect in comparison with center. The flow in annular cavity does not present this characteristic, because the vertical walls are different, in particular, when the curvature ratio increase. We can remark that the cell near the external wall move near the high right corner, while the one who is near the internal wall try to disappear (Fig. 6a). We observe also that the flow is speedy along the internal cylinder than the external cylinder at  $N = 2$  (Fig. 5).

The vertical wall with large surface (external wall) create the thick thermal and solutal boundary layers than the reduce surface (internal wall), it follows that the dynamics boundary layer is large along the external cylinder than the internal one. Which flow conservation corresponds at the high velocity where the boundary layer is thick.

Non-symmetric aspect in comparison with center of cavity for  $K > 1$  is observed also in thermal and

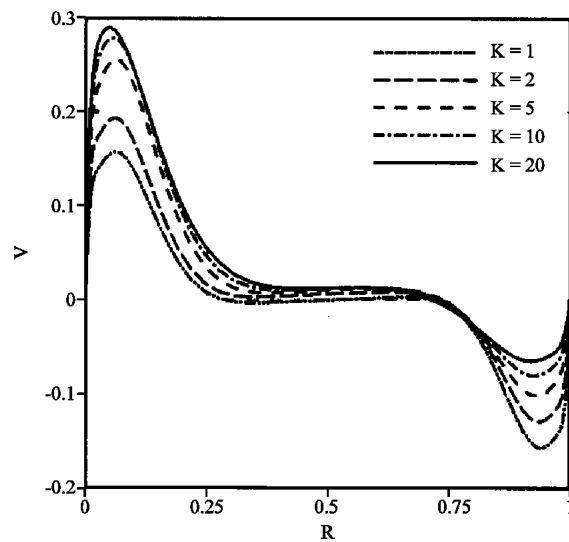


Fig. 5: Radial velocity profile at  $Y = 0.5$  (for  $Ra_t = 10^5$ ,  $Le = 100$ ,  $Pr = 7.0$ ,  $N = 2$ )

concentration field (Fig. 6b, c). In particular, the temperature in the center is not equal zero like the rectangular case ( $K = 1$ ), but it is near to the temperature of the large wall in proportion that the curvature ratio increase. This remark is same of the concentration field.

In the limit for  $K \gg 1$  (example  $K = 20$ , the flow is comparable at the case of the cylinder in the fluid mixture with the uniform temperature and concentration. Prasad (1986), found this result also in a study of natural convection in a vertical porous annulus He was considered that from  $K = 10$ , the flow can be assimilate at the boundary layer along the vertical cylinder.

**Heat and mass transfer:** The effect of curvature ratio on heat and mass transfer,  $Nu_i$  and  $Sh_i$ , for a buoyancy ratio range of  $2 \leq N \leq 50$  can be examined in Fig. 7 and 8. Generally,  $Nu_i$  and  $Sh_i$  increase with  $K$  for constant  $N$ . However,  $Nu_i$  tend to be joined when  $K$  increase ( $K > 20$ )

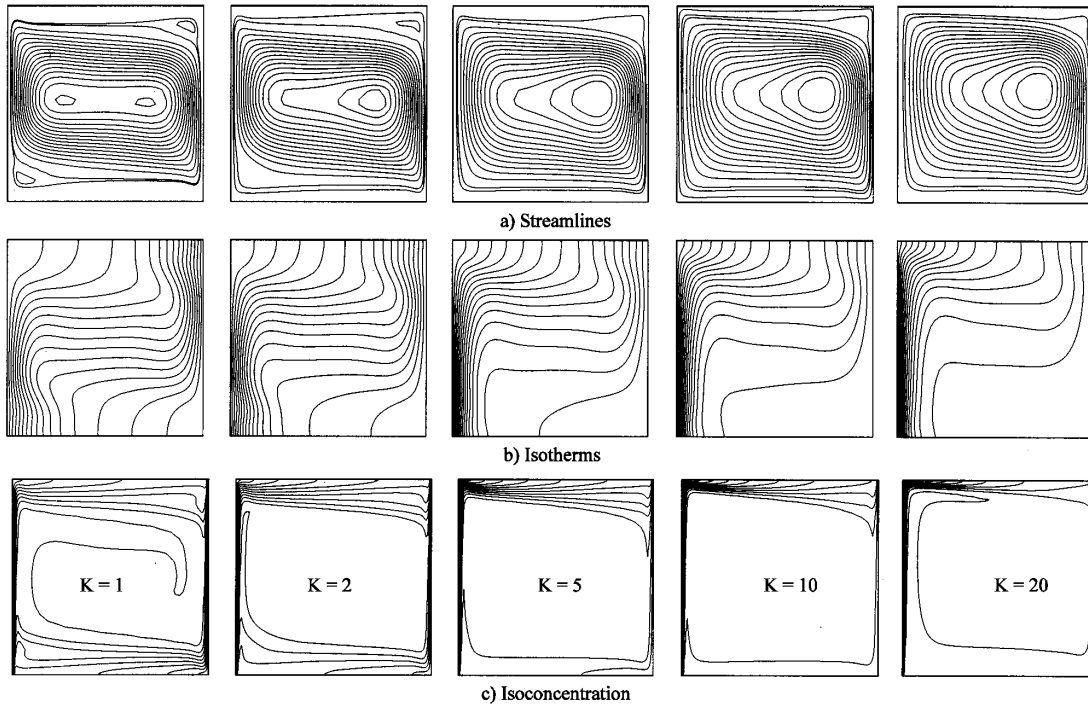


Fig. 6: Influence of the radii ratio ( $Pr = 7, Le = 100, N = 20, Ra_t = 10^5$ )

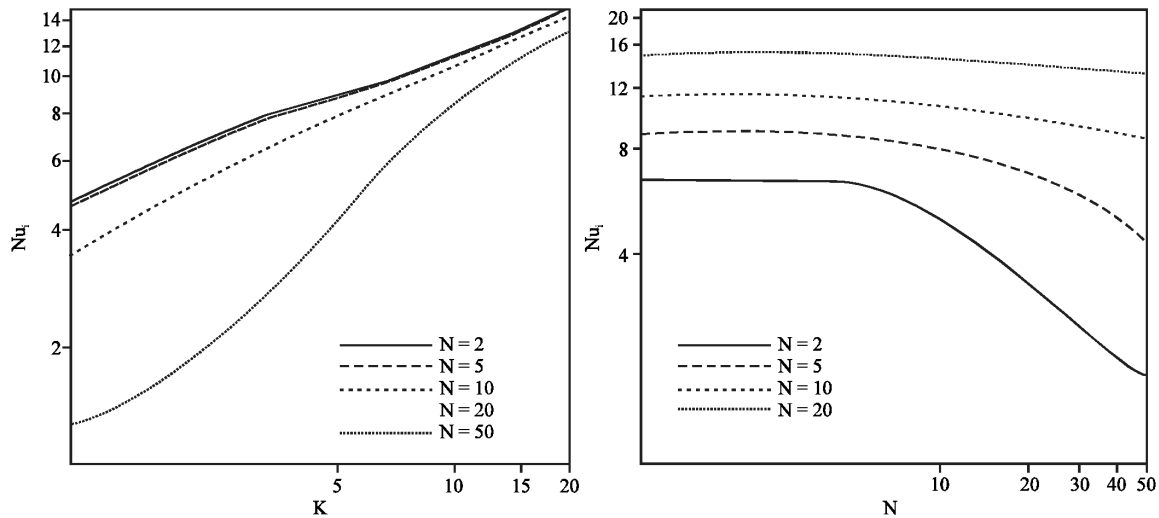


Fig. 7: Effect of  $K$  and  $N$  on  $Nu_t$  (for  $Ra_t = 10^5, Le = 100, Pr = 7.0$ )

for a buoyancy ratio range ( $2 \leq N \leq 50$ ) corresponding to constant  $Ra_t = 10^5$  for all that  $N$  increase. That is not the case to  $Sh_t$  where  $Ra_c$  become important when  $N$  increase (Fig. 7).

As a result  $Nu_t$  is observed to decrease considerably with  $N$  ( $Ra_t = 10^5$  and  $5 \times 10^5 \leq Ra_c \leq 5 \times 10^6$ ), when  $K = 2$  and  $K = 5$ . But when  $K$  is important ( $K = 10$  and  $K = 20$ ) this effect is not significantly.

Examining Fig. 8 reveals that spacing between curves  $Nu_t$  and  $Sh_t$  decrease when  $K$  increase because the effect of curvature ratio tend to be neglected and the flow can be assimilate at the boundary layer along the vertical cylinder.

We obtained some results in good concordance with the works of Shipp *et al.* (1993b) where they studied the effects of thermal Rayleigh number and Lewis number on

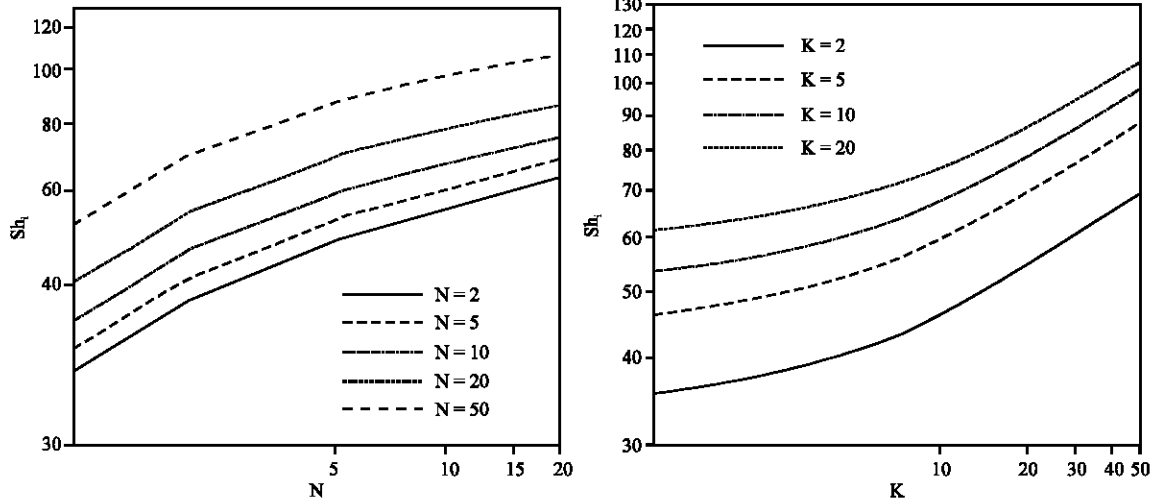


Fig. 8: Effect of K and N on  $Sh_i$  (for  $Ra_r = 10^5$ ,  $Le = 100$ ,  $Pr = 7.0$ )

double-diffusive natural convection in a closed annulus. Our results indicate that when the buoyancy ratio N increase, the mass transfer increases, on the other hand for any number of Lewis. The heat transfer increase when the number of Lewis is weak but when it is great than 10 the heat transfer decreases as the buoyancy ratio N increases. We found same results with a Lewis number equal to 100 where the Sherwood number increases and the Nusselt number decreases when the buoyancy ratio increases.

The non regular variation type of the Nusselt number and the Sherwood number (Fig. 7 and 8) didn't allow us to give some correlations to the heat and mass transfer.

**CONCLUSIONS**

This numerical study has for main objective to obtain original results in double-diffusive natural convection domain. The effect of buoyancy ratio and curvature ratio on the flow structure, the temperature and concentration distribution and the resulting heat and mass transfer rates is presented. The relationship for buoyancy ratios and average Nusselt and Sherwood numbers have been obtained for aiding flow at thermal Rayleigh number of  $10^5$  and a Lewis number of 100 in a vertical closed annulus with a binary mixture. The previous works studied either of the cases with weak Lewis numbers or great numbers of Lewis but in porous medium.

Numerical results are reported for laminar, double-diffusive, natural convection of a fluid in a closed vertical annulus cavity with an uniform temperature and concentration difference applied across the vertical walls. Conditions of aiding buoyancy forces are examined. The study concerns the double diffusive

convection phenomena under different geometrical conditions ( $1 \leq K \leq 20$ ) and different dynamical conditions ( $2 \leq N \leq 50$ ).

The results show that the heat transfer rate at high Lewis numbers behaves in a special manner, since it decreases with increasing of the buoyancy ratio. This has been shown to be due to the development of stratified zones in the top and bottom parts of the cavity where velocity gradients are negligible and the heat transfer is mainly driven by diffusion.

Under certain geometrical and dynamical conditions, the stratified flow zones are destabilized. Three thermosolutal convection flow regime have been obtained as a function of the buoyancy ratio N:

- At low buoyancy ratio, the flow exhibits a unicellular structure. The convection is dominated by the thermal effect.
- At moderate buoyancy ratio, a multicellular flow regime where thermal and solutal effects are comparable.
- At high buoyancy ratio, the flow exhibits a unicellular regime dominated by the solutal effect.

The numerical results show that the symmetric aspect is absent in the annular cavities in comparison with the rectangular case, in particular when the curvature ratio increase and the limit for  $K \gg 1$ , the flow is comparable at the case of the cylinder.

Unfortunately, no analytical or experimental results are available for a problem of this configuration; thus, it is not possible to make a direct comparison with the numerical results.



**Nomenclature**

- Ar : Aspect ratio ( $=H/\Delta r$ )
- C : Mass fraction of constituent
- D : Mass diffusivity of constituent through the fluid mixture
- g : Gravitational acceleration
- H : Height of enclosure
- K : Curvature ratio ( $=r_o/r_i$ )
- Le : Lewis number
- N : Buoyancy ratio [ $= (\beta_c \Delta C)/(\beta_T \Delta T)$ ]
- Nu : Nusselt number
- p : Pressure
- P : Dimensionless pressure [ $=(\Delta r^{2p})/(\rho \alpha^2 Ra_c)$ ]
- Pr : Prandtl number
- r : Radial coordinate
- R : Dimensionless radial coordinate [ $=(r-r_i)/\Delta r$ ]
- $Ra_c$  : Solutal rayleigh number [ $=(g \beta_c w \Delta C \Delta r^3)/(v \alpha)$ ]
- $Ra_T$  : Thermal rayleigh number [ $=(g \beta_T \Delta T \Delta r^3)/(v \alpha)$ ]
- S : Dimensionless concentration [ $=(C-C_i)/(C_i-C_o)$ ]
- Sh : Sherwood Number
- T : Dimensionless temperature [ $=(\theta-\theta_i)/(\theta_i-\theta_o)$ ]
- u : Radial velocity
- U : Dimensionless radial velocity
- v : Axial velocity
- V : Dimensionless axial velocity
- y : Axial coordinate
- Y : Dimensionless axial coordinate

*Greeks Symbols*

- $\alpha$  : Thermal diffusivity
- $\beta_c$  : Mass species expansion coefficient
- $\beta_T$  : Thermal expansion coefficient
- $\lambda$  : Thermal conductivity
- $\nu$  : Kinematics viscosity
- $\theta$  : Temperature
- $\rho$  : Fluid density

*Indices*

- c : Mass species
- i : Inner radial wall
- o : Outer radial wall
- r : Reference
- t : Thermal

**REFERENCES**

Bahloul, A., M. Yahiaoui, P. Vasseur, R. Bennacer and H. Beji, 2006. Natural convection of a two-component fluid in porous media bounded by tall concentric vertical cylinders. *J. Applied Mechan.*, 73: 26-33.

Bejan, A., 1985. Mass and heat transfer by natural convection in a vertical cavity: *J. Heat Fluid Flow*, 6: 149-159.

Bennacer, R. and D. Gobin, 1996. Cooperating thermosolutal convection in enclosures. -I. Scale analysis and mass transfer. *Intl. J. Heat Mass Transfer*, 39: 2971-2681.

Bennacer, R., H. Beji, R. Duval and P. Vasseur, 2000. The brinkman model for thermosolutal convection in a vertical annular porous layer. *Intl. Commun. Heat Mass Transfer*, 27: 69-80.

Gebhart, B. and L. Pera, 1971. The nature of vertical natural convection flows resulting from the combined buoyancy effects of thermal and mass diffusion. *Intl. J. Heat Mass Transfer*, 14: 2025-2050.

Gobin, D. and R. Bennacer, 1996. Cooperating thermosolutal convection in enclosures -II. Heat transfer and flow structure. *Intl. J. Heat Mass Transfer*, 39: 2983-2697.

Han, H. and T.H. Kuehn, 1991. Double diffusive natural convection in a vertical rectangular enclosure. Part I: Experimental study. *Intl. J. Heat Mass Transfer*, 34: 449-460.

Kamotani, Y., L.W. Wang, S. Ostrach and H.D. Jiang, 1985. Experimental study of natural convection in shallow enclosures with horizontal temperature and concentration gradients. *Intl. J. Heat Mass Transfer*, 28: 165-173.

Le Quere, P., 1987. Etude de la Transition à l'Instationarité des Ecoulements de Convection Naturelle en Cavité Verticale Différentiellement Chauffée par Methodes Spectrales Chebyshev, Ph.D. Thesis. University of Poitiers, France.

Lin, T.F., C.C. Huang and T.S. Chang, 1990. Transient binary mixture natural convection in square enclosure. *Intl. J. Heat Mass Transfer*, 33: 287-299.

Patankar, S.V., 1980. *Numerical Heat Transfer and Fluid Flow*. Hemisphere, Washington.

Prasad, V., 1986. Numerical study of natural convection in a vertical, porous annulus with constant heat flux on the inner wall. *Intl. J. Heat Mass Transfer*, 29: 841-853.

Retiel, N., 1995. Etude numérique de la convection thermosolutale en cavité annulaire. Solutions stationnaires et instationnaires. Ph.D Thesis, The University of Poitiers, France.

Shipp, P.W., M. Shoukri and M.B. Carver, 1993a. Double-diffusive natural convection in a closed annulus. *Numerical Heat Transfer, Part A*, 24: 339-356.

Shipp, P.W., M. Shoukri and M.B. Carver, 1993b. Effect of thermal rayleigh and lewis numbers on double-diffusive natural convection in a closed annulus. *J. Numerical Heat Transfer, Part A*, 24: 451-465.